THE JOURNAL OF PHYSICAL CHEMISTRY B

Article

pubs.acs.org/JPCB

Polarization versus Temperature in Pyridinium Ionic Liquids

Vitaly V. Chaban*[,†,‡] and Oleg V. Prezhdo[†]

[†]MEMPHYS - Center for Biomembrane Physics, Syddansk Universitet, Odense M, 5230, Kingdom of Denmark

[‡]Department of Chemistry, University of Southern California, Los Angeles, California 90089, United States

ABSTRACT: Electronic polarization and charge transfer effects play a crucial role in thermodynamic, structural, and transport properties of room-temperature ionic liquids (RTILs). These nonadditive interactions constitute a useful tool for tuning physical chemical behavior of RTILs. Polarization and charge transfer generally decay as temperature increases, although their presence should be expected over an entire condensed state temperature range. For the first time, we use three popular pyridinium-based RTILs to investigate temperature dependence of electronic polarization in RTILs, based on a nonperiodic electronic density description for a cation−anion pair. Atom-centered density matrix propagation molecular dynamics, supplemented by a weak coupling to an external bath, is used to simulate the temperature impact on system properties. We show that, quite surprisingly, nonadditivity in the cation−anion interactions changes negligibly between 300 and 900 K, while the average dipole moment increases due to thermal fluctuations of geometries. Our results contribute to the fundamental understanding of electronic effects in the condensed phase of ionic systems and foster progress in physical chemistry and engineering.

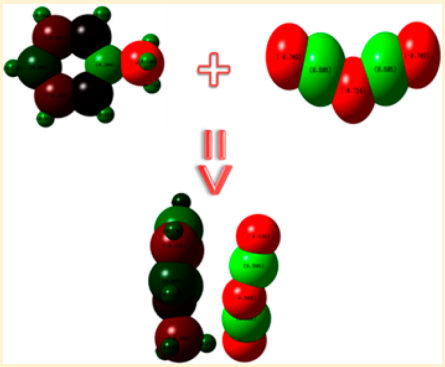

1. INTRODUCTION

Room-temperature ionic liquids (RTILs)[1−11] constitute an active research field. Applications of RTILs range from high-performance electrolyte solutions[1] to green solvents[12,13] to synthesis and separation setups.[5] Gas capture using ionic liquids stays somewhat apart from the mainstream efforts.[2] RTILs are famous for exhibiting extremely wide liquid temperature ranges, while preserving low volatility even at hundreds of degrees Celsius.[10] In turn, certain RTILs remain liquid well below the normal melting point of ice. It is, therefore, important to understand correlation between molecular level organization of these compounds and their macroscopic properties.

Nonadditive interactions, such as electronic polarization of a cation by an anion and charge transfer between these species, heavily influence physical properties of most ionic liquids.[14,15] Polarizable molecular dynamics (MD) simulations emerge in this context as a natural theoretical requirement for a better description of the strong interparticle binding in these ionic systems.[16−18] Typical RTILs present very slow dynamics, low ionic conductivity, and high viscosity. In addition, structural and dynamical heterogeneities at room temperature distinguish microscopic arrangements of ordinary molecular liquids and RTILs.[10,17]

Although nonadditive nonbonding interactions in the condensed state of RTILs have been addressed before, their dependence on temperature is unknown. The phenomenon has a crucial impact on the phase diagram of RTILs and numerous phase-dependent physical−chemical properties. Our work, for the first time, analyzes electronic polarization as a function of temperature for three pyridinium-based RTILs. Quite surprisingly, we find that temperature has little impact on electron delocalization, while it does influence dipole moments of ion pairs. The dipoles grow because of thermal expansion and geometry fluctuations. The study indicates that polarization and charge transfer should be properly represented in simulations of RTILs over the whole temperature range corresponding to the liquid state.

2. SIMULATION METHODOLOGY

The electronic energy levels and their populations were obtained for ion pairs of the pyridinium-based ionic liquids methylpyridinium chloride [PY][Cl], methylpyridinium tetrafluoroborate [PY][BF_4], and methylpyridinium dicyanamide, [PY][$N(CN)_2$], with nonperiodic density functional theory (DFT) using the BLYP functional.[19,20] BLYP is a well-established, reliable exchange-correlation functional in the generalized gradient approximation. The wave function was expanded using the effective-core LANL2DZ basis set developed by Dunning and co-workers.[21] This basis provides a reasonable trade-off between accuracy and computational expense, suitable for MD simulations with average-size systems. The wave function convergence criterion was set to 10^{-8} Hartree for all calculations. Table 1 presents the basic properties of the systems.

More accurate calculations would require a larger basis set and a hybrid DFT functional. Pure DFT functionals, such as BLYP, tend to overestimate electronic polarization by favoring delocalized electrons. The use of the moderate size basis set counteracts this tendency. Further, our calculations show that temperature has a minor impact on electron delocalization. By

Received: September 4, 2014
Revised: October 28, 2014
Published: November 11, 2014

dx.doi.org/10.1021/jp5089788 | J. Phys. Chem. B 2014, 118, 13940−13945

Table 1. Simulated Systems and Selected Results

system	no. electrons	no. basis functions	reference temperature, K	dipole moment, D	charge on cation, e
[PY][Cl]	58	393	300	8.6	0.52
[PY][Cl]	58	393	500	9.7	0.54
[PY][Cl]	58	393	900	10.8	0.54
[PY][BF_4]	92	580	300	12.5	0.82
[PY][BF_4]	92	580	500	13.2	0.82
[PY][BF_4]	92	580	900	16.5	0.80
[PY][$N(CN)_2$]	84	580	300	11.2	0.74
[PY][$N(CN)_2$]	84	580	500	11.8	0.71
[PY][$N(CN)_2$]	84	580	900	13.0	0.71

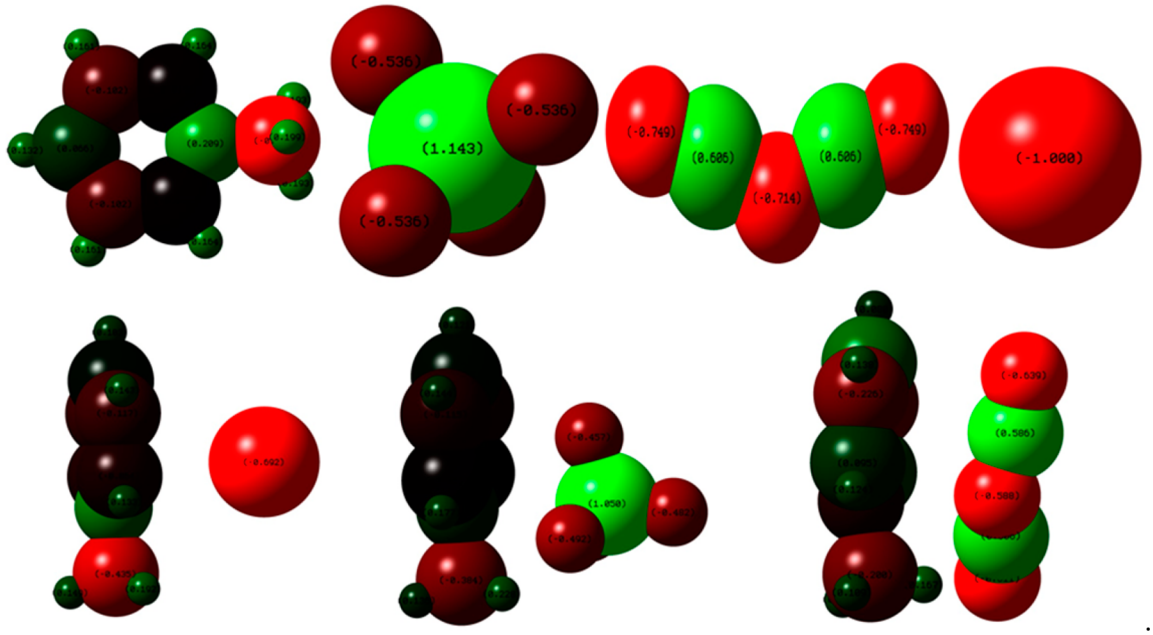

Figure 1. Distribution of partial electrostatic charges over the pyridinium cation and the selected anions. The depicted charges have been computed using the CHELPG fitting scheme.[25] The fitting was constrained to reproduce the dipole moments computed from the DFT electron density. Electron-rich atoms are shown in red, electron-poor atoms are shown in green, and nearly neutral/neutral atoms are shown in gray/black. The colors are more intense for larger partial charges.

overestimating electron delocalization, pure DFT functionals should also overestimate temperature-induced changes in delocalization. Hence, more rigorous and computationally intense calculations with hybrid functionals should confirm our conclusion.

Atom-centered density matrix propagation (ADMP) MD was simulated for 10 ps at 300, 500, and 900 K for the three selected RTIL systems (Table 1). The method computes a classical nuclear trajectory by propagating electron density with auxiliary degrees of freedom. The self-consistent field procedure used every time-step in Born–Oppenheimer MD is avoided. ADMP MD[22] performs somewhat better than Born–Oppenheimer MD in most cases, especially for relatively large systems and complicated convergence cases. It is not necessary in ADMP MD to use pseudopotentials on hydrogen atoms or substitute hydrogen atoms by deuterium atoms to increase the nuclear time-step.[22] Preservation of adiabaticity during dynamics should be controlled. In our calculations, the nuclear time-step of 0.1 fs was used at all temperatures. The fictitious electron mass was set to 0.1 a.m.u. On the basis of extensive preliminary tests, including variations in the nuclear time-step from 0.05 to 0.3 fs, the mass for the electron degrees of freedom from 0.05 to 0.6 a.m.u., and hydrogen isotopes, the present setup provides the best balance between electron–nuclear adiabaticity and fast propagation of the equations-of-motion. The functions of core electrons carried larger weights than those of valence electrons.

Each system was equilibrated for 1 ps to the desired temperatures by velocity rescaling. Next, 10 ps production trajectories were generated. In principle, thermostatting can be turned off after equilibration, and the subsequent simulation can be carried out in the microcanonical ensemble. Due to the small system size, and consequently, large temperature fluctuation, we compared the real and target temperatures every 5.0 fs during the production runs, and rescaled the velocities if the difference exceeded 50 K. The three systems were studied at the three different temperatures (Table 1), resulting in 90 ps of equilibrium trajectory data and 900 000 time-steps of nuclear motion. Sampling of rare conformations of the RTIL ion pairs extends beyond our simulation schedule. This may be the reason we did not observe sporadical ion pair configurations with negligible to no charge transfer, according to Hunt and co-workers.[23]

The atomic charges and ion pair dipole moments were generated along the MD trajectories using the Hirshfeld scheme.[24] The electrostatic potentials (ESPs) were obtained for

dx.doi.org/10.1021/jp5089788 | J. Phys. Chem. B 2014, 118, 13940–13945

optimized system geometries. The ESP derived from the electronic structure was reproduced using a set of point charges centered on each atom, including hydrogen atoms. The atom spheres were defined according to the CHELPG scheme.[25] Figure 1 depicts the optimized geometries (0 K) of isolated ions and ion pairs. The atoms are colored according to their polarity.

It is important to note that even though only a single ion pair is simulated per system, the considered interactions take place among numerous electrons and nuclei. Hence, the interactions and discussed effects are many-body and generally nonadditive.

The electronic structure computations were performed using GAUSSIAN 09, revision D. The subsequent analysis was performed using utilities developed by V.V.C.

3. RESULTS AND DISCUSSION

The anions are chosen to represent a variety of structures. Cl^- has high charge density and is capable of significantly polarizing surrounding species. Ionic liquids containing Cl^- are strongly electrostatically driven and, therefore, exhibit relatively high melting points. Similarly to Cl^-, BF_4^- is a spherical particle, but with a different distribution of electrons. In turn, $N(CN)_2^-$ features a unique structure with two chemically nonequivalent nitrogen atoms and a symmetry, which may or may not be broken in the condensed phase. The anions with more delocalized excess electronic charge are beyond the scope of the present work, since their polarizing ability is generally weaker. The cation is represented by methylpyridinium, PY^+. Pyridinium cations used in practice possess longer hydrocarbon chains (for instance, *N*-butylpyridinium). Our choice is made in the view of computational limitations of DFT. Electrically neutral hydrocarbon chains neither polarize the central fragment of the cation, nor get polarized by the anion. Pyridinium-based ionic liquids are vigorously investigated nowadays due to their versatility and tunable properties.[26−30]

Table 1 introduces the simulated systems, and their most important parameters and properties. Interestingly, the methyl carbon atom is the most electron deficient atom in the isolated methylpyridinium cation (−0.4 e), while all other cation atoms are essentially neutral. The nitrogen atom is only slightly positive, +0.2 e. Therefore, one expects that the anion species are coordinated by these two bonded atoms. The boron atom of the tetrafluoroborate anion is +1.143 e, compensated by the fluorine atoms, −0.536 e each. Note that the computed electrostatic point charges at BF_4^- are in excellent agreement with those used in the classical force fields to reproduce electrostatic nonbonded interactions.[17,18] This fact indicates that our electronic structure calculations give reliable results. The central nitrogen atom of $N(CN)_2^-$ is not symmetrically equivalent to the nitrogen atoms of the two cyan groups. It should be stressed that all three nitrogen atoms carry anion's negative charge, whereas the two carbon atoms are positive, partially compensating the negative charge. Because all three nitrogens are negative, the excess electron is delocalized, in contrast to chloride. On the basis of the difference in electronegativity between carbon and nitrogen, one expected a smaller difference in their partial electrostatic charges. As expected, coordination of all anions occurs through the nitrogen atom of the pyridine ring and the methyl group. If longer alkyl chains had been used, the positive charge would not have been localized so much on the methyl carbon atom, and the coordination center would have shifted toward the nitrogen atom.

Partial insights into electron polarization and transfer can be obtained from localization of valence orbitals, in particular the highest occupied (HOMO) and lowest unoccupied (LUMO) molecular orbitals of the ion pair (Figure 2). Polarization effects

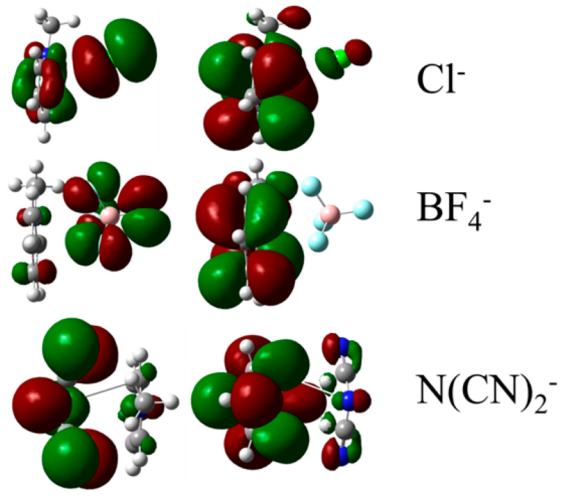

Figure 2. Highest occupied molecular orbitals (HOMO, left) and lowest unoccupied molecular orbitals (LUMO, right) in methylpyridinium chloride (Cl^-), tetrafluoborate (BF_4^-), and dicyanamide ($N(CN)_2^-$).

can be viewed as partial excitation of electron from occupied to vacant orbitals. Both the HOMO and the LUMO are delocalized over the [PY][Cl] ions. In the case of [PY][BF_4], the HOMO is localized on the anion, while the LUMO is on the cation. Excitation from the HOMO to the LUMO results in electron transfer from the anion to the cation. The HOMO and the LUMO of [PY][$N(CN)_2$] are mostly on the anion, but they are not perfectly localized. The analysis of higher-energy orbitals of the ion pairs suggests a strong noncovalent interaction (mostly electrostatic attraction) with evident nonadditive phenomena. In some cases, polarization effects extend beyond the HOMO−LUMO analysis, and require consideration of other orbitals. For instance, the HOMO is localized on the anion and the LUMO is localized on the cation in the PY/BF_4 ion pair, while both the HOMO and the LUMO are localized on the anion in the PY/$N(CN)_2$ pair. This should lead to better stabilization of the negative charge on the $N(CN)_2$ anion compared to BF_4. Therefore, the $N(CN)_2$ anion should have less charge transfer to PY, which is at odds with the charge analysis.

Further insights can be derived by comparing the total electronic density in the ion pair to the total electronic density of lone ions. Ghost basis functions must be present to avoid artifacts. These possible artifacts are connected with basis set superposition, upon consideration of lone ions in the same conformations as they are in the optimized geometry of the ion pair. Note that the results of Figures 1 and 2 correspond to the electronic structures of cold (0 K) conformations, obtained after geometry optimization. It is difficult to uniquely distinguish the polarization and charge transfer effects in the case of polyatomic chemical formations. Intramolecular charge transfer can occur in addition to polarization and charge transfer between the anion and the cation. The present work primarily focuses on the integrated nonadditive effects as a function of temperature.

dx.doi.org/10.1021/jp5089788 | J. Phys. Chem. B 2014, 118, 13940−13945

Thermal fluctuations of the total electrostatic partial charge localized on the pyridine ring are plotted in Figure 3 for the

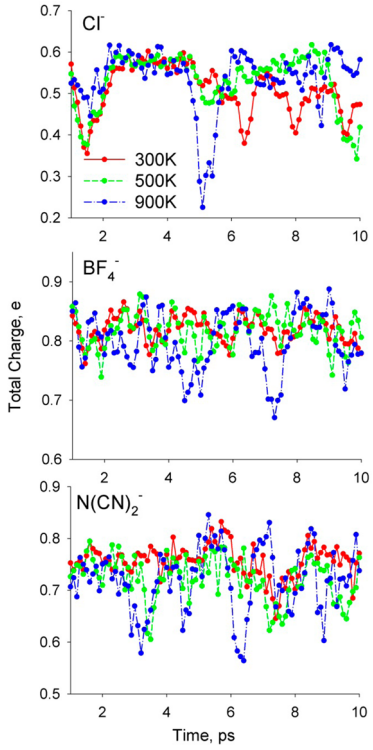

Figure 3. Fluctuation in the positive charge localized on the pyridine ring of the cation in the presence of the Cl^-, BF_4^-, and $N(CN)_2^-$ anions: 300 K (red solid line), 500 K (green dashed line), and 900 K (blue dash-dotted line). Electron partitioning between the atoms is based on the Hirshfeld procedure.[24]

three RTILs at the three studied temperatures. Huge fluctuations are observed, with fluctuation amplitude in direct proportion to temperature. For instance, at 900 K, the sum of Hirshfeld charges[24] on the cation in [PY][Cl] drops to nearly 0.2 e, but then quickly returns to the equilibrium value of 0.54 e. No drift in time is observed for this property, suggesting that all systems are properly equilibrated. Surprisingly, the average values are almost independent of temperature (Table 1, Figure 4). This is unexpected, since specific cation−anion interactions tend to decay as temperature increases. A 600 K temperature increase from 300 to 900 K is quite significant to expect changes. To exclude the possibility that the lack of the

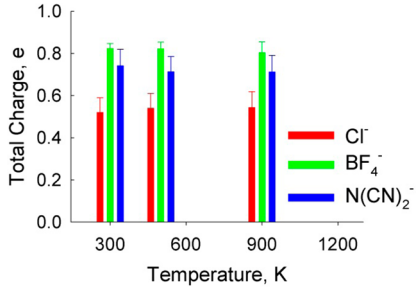

Figure 4. Canonically averaged values of the positive charge localized on the pyridine ring of the cation for different temperatures and anions. Electron partitioning between the atoms is based on the Hirshfeld procedure.[24]

temperature impact arises because the simulated systems are small, leading to a large uncertainty in the actual temperature, we performed additional simulations using four ion pairs. However, the conclusion did not change. The canonically averaged charges are nearly independent of temperature, however, the magnitude of the fluctuations around the average value is proportional to temperature.

The temperature-induced change in the negative charge of the chloride anion is within the 0.52−0.54 e range. The changes in the negative charges of BF_4^- and $N(CN)_2^-$ are 0.80−0.82 e and 0.71−0.74 e, respectively. We hypothesize that insensitivity to temperature comes from genuinely strong noncovalent interactions in these systems. The cation−anion binding energy well exceeds the kinetic energy in the binding coordinate. All ions remained chemically stable during 10 ps of the simulated nuclear dynamics, but this time period may be too short to observe a decomposition reaction.

Dipole moment (Figure 5) provides an alternative description of electric properties, as it characterizes not only

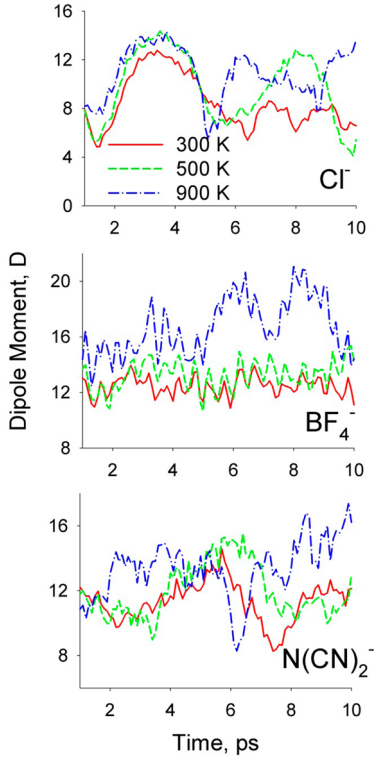

Figure 5. Evolution of the dipole moment of the ion pair containing pyridinium cation at various temperatures: 300 K (red solid line), 500 K (green dashed line), and 900 K (blue dash-dotted line).

atomic charges, but also separation of positive and negative centers-of-mass of the electron−nuclear system. Dipole moments of the ion pairs of the pyridinium-based RTILs increase significantly with temperature (Table 1). The largest dipole moment of 16.5 D is observed for $[PY][BF_4]$ at 900 K. The dipole moments of [PY][Cl] are systematically smaller at all temperatures: 8.6 D (300 K), 9.7 D (500 K), 10.8 D (900 K). The observed growth of dipole moments with temperature leads to increase in the dielectric constant of these RTILs in the condensed phase.

dx.doi.org/10.1021/jp5089788 | J. Phys. Chem. B 2014, 118, 13940−13945

4. CONCLUDING REMARKS

We have shown that temperature has a very minor impact on electron delocalization in the pyridinium-based RTIL ion pairs, which is a rather unexpected result. At the same time, dipole moments increase systematically upon RTIL heating due to growing thermal fluctuations of the corresponding structures and thermal expansion. Because electronic polarization and charge transfer effects do not decay with temperature, they must be properly accounted for in simulations of condensed phase ionic liquids.

The provided analysis is based on ion pairs simulated in vacuum rather than condensed phase. This is due to a set of methodological restrictions. First, computational cost for simulations of quantum dynamics is often prohibitive for systems of more than a few hundred electrons. Second, computation of the long-range electrostatic potential is not straightforward in periodic systems. In addition, point charges cannot be univocally defined far from the surface of an ion cluster/aggregate ("buried atom" problem). Third, the dipole moment is most meaningful in the case of a single ion pair, whereas higher-order electric moments suit better for description of large molecular formations. We expect that periodic systems would have electron densities on each atom slightly different from those computed here for the ion pairs. Nevertheless, the qualitative conclusions of this work should not change. In the condensed phase, ion pairs would dominate over more complicated ionic aggregates. Such systems exhibit a well-defined first peak in the radial distribution functions, but much less structured second and possibly third peaks. If a single cation−anion coordination site prevails, as it is anticipated in this case, introduction of additional ions will not change the observables qualitatively.

AUTHOR INFORMATION

Corresponding Author

*E-mail: vvchaban@gmail.com; chaban@sdu.dk.

Notes

The authors declare no competing financial interest.

ACKNOWLEDGMENTS

This research has been supported by grant CHE-1300118 from the U.S. National Science Foundation. MEMPHYS, the Danish National Center of Excellence for Biomembrane Physics, is supported by the Danish National Research Foundation.

REFERENCES

(1) Fedorov, M. V.; Kornyshev, A. A. Ionic Liquids at Electrified Interfaces. *Chem. Rev.* **2014**, *114*, 2978−3036.
(2) Brennecke, J. E.; Gurkan, B. E. Ionic Liquids for CO_2 Capture and Emission Reduction. *J. Phys. Chem. Lett.* **2010**, *1*, 3459−3464.
(3) Lei, Z. G.; Dai, C. N.; Chen, B. H. Gas Solubility in Ionic Liquids. *Chem. Rev.* **2014**, *114*, 1289−1326.
(4) Ren, Z.; Ivanova, A. S.; Couchot-Vore, D.; Garrett-Roe, S. Ultrafast Structure and Dynamics in Ionic Liquids: 2D-IR Spectroscopy Probes the Molecular Origin of Viscosity. *J. Phys. Chem. Lett.* **2014**, *5*, 1541−1546.
(5) Hallett, J. P.; Welton, T. Room-Temperature Ionic Liquids: Solvents for Synthesis and Catalysis. 2. *Chem. Rev.* **2011**, *111*, 3508−3576.
(6) van Rantwijk, F.; Sheldon, R. A. Biocatalysis in Ionic Liquids. *Chem. Rev.* **2007**, *107*, 2757−2785.
(7) Luo, X. Y.; Ding, F.; Lin, W. J.; Qi, Y. Q.; Li, H. R.; Wang, C. M. Efficient and Energy-Saving CO_2 Capture through the Entropic Effect Induced by the Intermolecular Hydrogen Bonding in Anion-Functionalized Ionic Liquids. *J. Phys. Chem. Lett.* **2014**, *5*, 381−386.
(8) Zhang, X. X.; Liang, M.; Ernsting, N. P.; Maroncelli, M. Conductivity and Solvation Dynamics in Ionic Liquids. *J. Phys. Chem. Lett.* **2013**, *4*, 1205−1210.
(9) Hettige, J. J.; Kashyap, H. K.; Annapureddy, H. V. R.; Margulis, C. J. Anions, the Reporters of Structure in Ionic Liquids. *J. Phys. Chem. Lett.* **2013**, *4*, 105−110.
(10) Chaban, V. V.; Prezhdo, O. V. Ionic and Molecular Liquids: Working Together for Robust Engineering. *J. Phys. Chem. Lett.* **2013**, *4*, 1423−1431.
(11) Szefczyk, B.; Cordeiro, M. N. D. S. Physical Properties at the Base for the Development of an All-Atom Force Field for Ethylene Glycol. *J. Phys. Chem. B* **2011**, *115*, 3013−3019.
(12) Horvath, I. T.; Anastas, P. T. Innovations and Green Chemistry. *Chem. Rev.* **2007**, *107*, 2169−2173.
(13) Maciel, C.; Fileti, E. E. Molecular Interactions between Fullerene C-60 and Ionic Liquids. *Chem. Phys. Lett.* **2013**, *568*, 75−79.
(14) Chaban, V. Polarizability Versus Mobility: Atomistic Force Field for Ionic Liquids. *Phys. Chem. Chem. Phys.* **2011**, *13*, 16055−16062.
(15) Chaban, V. V.; Voroshylova, I. V.; Kalugin, O. N. A New Force Field Model for the Simulation of Transport Properties of Imidazolium-Based Ionic Liquids. *Phys. Chem. Chem. Phys.* **2011**, *13*, 7910−7920.
(16) Borodin, O. Polarizable Force Field Development and Molecular Dynamics Simulations of Ionic Liquids. *J. Phys. Chem. B* **2009**, *113*, 11463−11478.
(17) Lopes, J. N. C.; Padua, A. A. H. Cl&P: A Generic and Systematic Force Field for Ionic Liquids Modeling. *Theor. Chem. Acc.* **2012**, *131*, 1129.
(18) Salanne, M.; Rotenberg, B.; Jahn, S.; Vuilleumier, R.; Simon, C.; Madden, P. A. Including Many-Body Effects in Models for Ionic Liquids. *Theor. Chem. Acc.* **2012**, *131*, 1143.
(19) Becke, A. D.; Roussel, M. R. Exchange Holes in Inhomogeneous Systems - a Coordinate-Space Model. *Phys. Rev. A* **1989**, *39*, 3761−3767.
(20) Lee, C. T.; Yang, W. T.; Parr, R. G. Development of the Colle-Salvetti Correlation-Energy Formula into a Functional of the Electron-Density. *Phys. Rev. B* **1988**, *37*, 785−789.
(21) Dunning, T. H.; Hay, P. J. In *Modern Theoretical Chemistry*; Schaefer, H. F., III, Ed.; Plenum: New York, 1977; Vol. 3, pp 1−28.
(22) Schlegel, H. B.; Iyengar, S. S.; Li, X. S.; Millam, J. M.; Voth, G. A.; Scuseria, G. E.; Frisch, M. J. Ab Initio Molecular Dynamics: Propagating the Density Matrix with Gaussian Orbitals. III. Comparison with Born-Oppenheimer Dynamics. *J. Chem. Phys.* **2002**, *117*, 8694−8704.
(23) Hunt, P. A.; Kirchner, B.; Welton, T. Characterising the Electronic Structure of Ionic Liquids: An Examination of the 1-Butyl-3-Methylimidazolium Chloride Ion Pair. *Chem.—Eur. J.* **2006**, *12*, 6762−6775.
(24) Hirshfeld, F. L. Bonded-Atom Fragments for Describing Molecular Charge-Densities. *Theor. Chim. Acta* **1977**, *44*, 129−138.
(25) Breneman, C. M.; Wiberg, K. B. Determining Atom-Centered Monopoles from Molecular Electrostatic Potentials - the Need for High Sampling Density in Formamide Conformational-Analysis. *J. Comput. Chem.* **1990**, *11*, 361−373.
(26) Kim, M. J.; Shin, S. H.; Kim, Y. J.; Cheong, M.; Lee, J. S.; Kim, H. S. Role of Alkyl Group in the Aromatic Extraction Using Pyridinium-Based Ionic Liquids. *J. Phys. Chem. B* **2013**, *117*, 14827−14834.
(27) Oliveira, M. B.; Llovell, F.; Coutinho, J. A. P.; Vega, L. F. Modeling the [Ntf2] Pyridinium Ionic Liquids Family and Their Mixtures with the Soft Statistical Associating Fluid Theory Equation of State. *J. Phys. Chem. B* **2012**, *116*, 9089−9100.
(28) Aparicio, S.; Atilhan, M. Mixed Ionic Liquids: The Case of Pyridinium-Based Fluids. *J. Phys. Chem. B* **2012**, *116*, 2526−2537.
(29) Bandres, I.; Alcalde, R.; Lafuente, C.; Atilhan, M.; Aparicio, S. On the Viscosity of Pyridinium Based Ionic Liquids: An Experimental and Computational Study. *J. Phys. Chem. B* **2011**, *115*, 12499−12513.

(30) Fernandes, A. M.; Rocha, M. A. A.; Freire, M. G.; Marrucho, I. M.; Coutinho, J. A. P.; Santos, L. M. N. B. F. Evaluation of Cation-Anion Interaction Strength in Ionic Liquids. *J. Phys. Chem. B* **2011**, *115*, 4033−4041.